Water-based root exudates of Molinia caerulea (L.) Moench disrupt root nitrogen metabolism in Quercus petraea (Matt.) Liebl. seedlings with a fast negative effect on budburst

Larissa Adamik, Philippe Balandier, Jean-Stéphane Venisse, Marine Fernandez, Philippe Malagoli

Adamik *et al. Annals of Forest Science* (2025) 82:31
https://doi.org/10.1186/s13595-025-01306-6

INRAE

Annals of Forest Science

RESEARCH

Open Access

Water-based root exudates of *Molinia caerulea* (L.) Moench disrupt root nitrogen metabolism in *Quercus petraea* (Matt.) Liebl. seedlings with a fast negative effect on budburst

Larissa Adamik[1], Philippe Balandier[2], Jean-Stéphane Venisse[1], Marine Fernandez[1] and Philippe Malagoli[1*]

Abstract

Key message *Molinia caerulea* (L.) Moench has been observed to significantly reduce budburst in *Quercus petraea* (Matt.) Liebl. seedlings through water-based *M. caerulea* root exudates. This suggests direct allelopathic effects between the two species. In terms of nutrient uptake, oak roots primarily take up nitrogen in the forms of ammonium and glycine. Interestingly, the application of root exudates from *M. caerulea* doubled the nitrate uptake in oak roots. Moreover, gene sets involved in nitrogen metabolism within oak roots exhibited strong deregulation when treated with *M. caerulea* root exudate, indicating that the interaction between these two plant species alters the nitrogen metabolism in the oak roots.

Context Oak regeneration encounters numerous impediments, including interactions with *Molinia caerulea* (L.) Moench, an understory grass species widespread in temperate forests. Besides competition for resources, our previous work suggested that the interaction between oak and *M. caerulea* may involve allelopathic processes.

Aim This study tested the hypothesis that *M. caerulea* affects the budburst dynamics, early growth of oak seedlings, and root N uptake transport and assimilation systems.

Methods Potted oak seedlings (*Quercus petraea* (Matt.) Liebl.) were watered with *M. caerulea* root exudates or water for 6 weeks during April and May 2021. The capacity of oak seedlings to take up nitrogen in its main molecular forms was characterized by an influx analysis of isotopically labeled (^{15}N) nitrate, ammonium, and glycine on excised roots using the "teabag" technique. Concomitantly, targeted transcriptomics were carried out to monitor changes in gene expression related to nitrogen metabolism.

Results The treatment resulted in reduced budburst rates (− 50%), together with an early reduction in height increment. Kinetics of N influx rates revealed that ammonium, and to a lesser degree glycine, were the predominant forms in which N was taken up by roots. Application of *M. caerulea* root exudate barely increased the ammonium influx rate and had no effect on the glycine influx rate. By contrast, the nitrate influx rate, despite its low values, doubled

Handling editor: Erwin Dreyer

*Correspondence:
Philippe Malagoli
philippe.malagoli@uca.fr
Full list of author information is available at the end of the article

after application of the exudate. Targeted transcriptomic analysis revealed a regulatory shift in gene sets associated with key mechanisms underlying N uptake, assimilation, and long-distance transport in oak roots.

Conclusion Interactions between a perennial grass, *M. caerulea*, and a woody species, *Q. petraea*, do not only rely upon direct competition for resources. Allelopathic processes must be taken into consideration when designing regeneration operations.

Keywords Allelopathy, Phenology, Nitrogen, Root uptake, Assimilation, Transcriptome

1 Introduction

Natural oak regeneration has become difficult over the last three decades (Thomas et al. 2002), and oak planting remains a challenging alternative (Clark et al. 2016;Schuler and Robison, 2010).

Besides animal predation, seedbed properties, and disturbance, well-documented negative plant-plant interactions have helped to explain failure in forest regeneration (Hoffmann and Haridasan 2008; Mallik 2003; Nilsson and Zackrisson 1992; Shimoda et al. 1994; Watt 1919). Several studies have highlighted the inhibitory action of understory plant species on tree regeneration (Mallik 2003). Although classical competition for resources among species is well documented, allelopathic interactions remain less understood. Physiological processes specifically targeted by allelochemicals are poorly identified. In temperate oak forests, *Molinia caerulea* (L.) Moench, a moor grass occurring on temporarily waterlogged acid soils, has been recognized as an important interfering species (Fernandez et al. 2022). Over 73% of biomass loss was recorded in *Quercus rubra* L. seedlings when growing with *M. caerulea* in non-fertilized systems (Timbal et al. 1990).

M. caerulea easily outcompetes temperate oak seedlings through its ability to quickly monopolize resources such as light, water, and nitrogen (Vernay et al. 2016, 2019). In forest environments, nitrogen (N) economy is a crucial factor for plant development (Fernandez et al. 2022). Vernay et al. (2016) observed limited N uptake by oak roots when oak was mixed-grown with *M. caerulea*. Findings from Fernandez et al. (2020, 2021) showed not only enhanced rhizodeposition from oak seedlings but also facilitated N transfer from oak to *M. caerulea*. Furthermore, *M. caerulea* is known to display an inhibitory allelopathic action on oak (Becker and Levy 1983; Fernandez et al. 2022; Weise 1960), although the responsible bioactive chemicals have not yet been identified, and thus their physiological targets remain unknown. Competition, facilitation, and allelopathy offer a clear advantage for *M. caerulea* and partly explain its dominance over oak seedlings.

Previous characterization of nitrogen flux dynamics between these two species suggested that allelopathic action relied on decreased root N uptake in tree seedlings. Jabran et al. (2013) stated that allelopathic activity generally includes a decrease in plant root mineral uptake. This has been confirmed for nitrogen sources (Simon 2023; Warren and Adams 2007). Many allelochemicals are known to make nitrogen sources unavailable to the target plant. This may occur through actions on nitrification, ammonification, and N volatilization processes, by complexation with other elements in the soil (Zhang et al. 2021) or through inhibited nutrient root uptake, via reduced root growth and decreased nutrient transport system activity, and reduced nutrient use efficiency (Scavo et al. 2019). The non-negligible contribution of organic nitrogen to nutrition in tree species has gained greater recognition (Simon 2023). However, allelopathic action on organic nitrogen uptake has so far been scantly studied in forest ecosystems.

Regardless of the inorganic N forms, NH_4^+ is the primary cytosolic N substrate to be assimilated into numerous biomolecules via specific metabolism pathways. These are systemically reallocated in the plant through release in the vascular system. In this way, N content and its related metabolisms inside and/or outside plants are essential as regulatory signals and energy resources in the fine tuning of responses associated with plant adaptation to fluctuating environmental constraints, such as allelopathic stress.

At a physiological level, root nitrogen influx relies on activities of root transport systems specific to the chemical form of their substrates (Wang et al. 2012). Mineral transport takes place via two different transport systems depending on substrate concentrations in the soil solution: high affinity transport systems (HATS) function when substrate concentrations are low (typically 0.5–1 mM), while low affinity transport systems (LATS) take up substrate when their concentrations exceed 0.5–1 mM (Crawford and Glass 1998). At a molecular level, the root N uptake pathway relies on several NO_3^- transporters. These include the nitrate transporter NRT1/PTR, NRT2 and NAR2 with the chloride channel (CLC), and the S-type anion channels SLACs and their homologs SLAHs. NH_4^+ uptake is regulated by the ammonium transporters (AMTs), and the

aqua-ammoniaporins, which are specific major intrinsic proteins (MIPs) or aquaporins (AQPs).

The present work sets out to characterize root N uptake and N assimilation in oak seedlings in response to the application of root exudates from *M. caerulea*, assumed to convey allochemicals (Fernandez et al. 2021). We hypothesized that allelopathic compounds would decrease the activity of N transport systems targeting root N transporters and alter N metabolism pathways during spring regrowth. Indeed, at this stage, tree seedling development is particularly dependent on N resource availability, a resource that is crucial for bud and shoot growth (Thitithanakul et al. 2012; Millard and Grelet 2010). We hypothesized that changes in N metabolism in oak root due to interaction with *M. caerulea* may result in changed phenology in oak shoots. Accordingly, we investigated the shoot's phenological response (budburst phenology and early growth). Functional responses were studied by monitoring root N influx using ^{15}N labeling. This was extended by analyzing the expression of genes associated with N metabolism. We focused on key gene subfamilies involved in cellular uptake and N metabolism, encompassing enzymatic assimilation and intra- and intercellular fluxes of inorganic and organic N forms.

2 Materials and methods

2.1 Experimental site and plant material

All experiments were carried out at Clermont-Ferrand, France, 45° 77′ 3″ N, 3° 14′ 3″ E (394 m a.s.l.). *M. caerulea* was collected on January 27, 2021, from the French National Forest of Vierzon (47° 16′ 4″ N, 2° 07′ 1″ E). Plants were dug out along with the main parts of their root systems, and stored in plastic bags to maintain humidity during transport to the laboratory. On January 28, 2021, 60 tufts were individually potted in 10-L plastic pots. Concomitantly, 100 2-year-old *Q. petraea* seedlings from a tree nursery were potted (1 seedling per pot). The soil used for both species had a typical loam texture (sand 51%, silt 29%, clay 20%), with a pH_{water} of 5.95. The soil C:N ratio (9.2) indicated active decomposition. The total nitrogen content was 2.1 g kg^{-1}, indicating that N was not a limiting factor. Nitrogen content as ammonium was 32.1 mg kg^{-1}, and as nitrate 123 mg kg^{-1}. Phosphorus, potassium, and cation exchange capacities were not limiting.

2.2 Experimental design

From January 28 to April 07, 2021, plants were acclimated to pot environment before the onset of new growth, i.e., the beginning of the growing season. All plants were maintained under semi-natural conditions: the pots were left outdoors under natural light, temperature, and precipitation. Plants were potted separately to avoid resource-based interactions. Manual weeding was done as needed. Irrigation began in March to avoid any water limitation.

When first budbursts occurred in 30% of the oaks, from April 07, 2021, *M. caerulea* roots were dug out every week and a root exudate was prepared (see Section 2.3). The *M. caerulea* plants then had an average fresh weight of 41.6 ± 3.9 g. A volume of 60 mL of their exudates was used to water 50 randomly selected oak seedlings. The remaining 50 seedlings received the same volume of distilled water free from *M. caerulea* compounds, constituting the control group. The same volume of exudates was added once a week for 6 weeks. Treatment duration was chosen according to Fernandez et al. (2020), who observed an effect of exudates a few weeks after treatment began. All plants' shoot growth and leaf budburst were assessed.

After 6 weeks of treatment (the week of May 17, 2021), oak plants were depotted and separated into shoots and roots. Soils containing root systems were coarsely sifted using a sieve of 2 mm mesh diameter and roots were collected. Roots were then sorted according to diameter. From five randomly selected individuals per modality, fine roots with a diameter less than 1 mm were selected for N influx analysis (see below). All fine roots were kept under a cool humid atmosphere to retain uptake capacity (Lucash et al. 2007) before carrying out influx measurements a few hours after harvest on the same day (see Section 2.6). For transcriptomic experiments, from the same individuals sampled for influx analysis, one root sample was taken per oak seedling. Accordingly, for each biological condition (control and treatment with *M. carulea* exudate), five biological replicates were generated, each consisting of a mixture of six randomly selected seedlings. All were placed in liquid nitrogen and stored at – 80 °C until use (see Section 2.9).

2.3 Collection of *M. caerulea* root exudates

M. caerulea roots keep their capacity to exudate secondary metabolites into their environment several days after the shoots have been removed (Lucash et al. 2007). Intact roots from freshly de-earthed plants were squeezed and placed in clean hermetic 1-L lunch boxes containing distilled water in an amount such that the final ratio of dry weight to water volume (DWV) of the solution was 2%. Boxes were placed in the dark at 20–25 °C for 48 h, the mean time before roots become inactive (Lucash et al. 2007). Water exudates from *M. caerulea* roots were applied to pots containing oak to convey *M. caerulea* allelochemicals to oak roots.

2.4 Budburst and early growth of oaks

First appearance of a leaf in at least one bud was recorded as budburst (BBCH 09). Relative budburst rate for a given time t was computed at the treatment group scale as follows:

$$\text{Relative budburst rate}\ (t) = [\%\text{burst}(t) - \%\text{burst}(t-1)]/\%\text{burst}(t-1) \quad (1)$$

Budburst and growth of oak seedlings were monitored weekly, measuring maximal height of shoots during the treatment. Relative height increment (%) was calculated for each seedling to compare weekly changes:

$$\text{Relative height increment} = [\text{height}(t) - \text{height}(t-1)] \times 100/\text{height}(t-1) \quad (2)$$

2.5 Influx measurements for ^{15}N-nitrate, ^{15}N-ammonium, and ^{15}N-glycine in *Q. petraea* seedling roots

Root N uptake kinetics in treated and non-treated oak seedlings were established based on ^{15}N isotopic labeling of three different chemical forms, all contributing to N nutrition: mineral forms ($^{15}NO_3^-$ and $^{15}NH_4^+$) and an organic form (amino acid ^{15}N-glycine). Among amino acids, glycine was chosen because it is directly absorbed by trees (Warren and Adams 2007). Solutions with different nitrogen concentrations were prepared: 50 µM and 500 µM to assess high affinity transport systems (HATS) activity and 1500 µM for assessing low affinity transport systems (LATS) activity. For each combination of N form and concentration, the analysis was repeated using five different oak seedlings. First, 6 g of excised oak fine roots was placed in teabags and washed with 0.5 mM $CaSO_4$ solution for 30 min to rid roots of soil residues while maintaining membrane integrity (Boss and Mott 1980; Britto et al. 2000; Kronzucker et al. 1995a, 1995b). For acclimation, roots were then placed for 1 h in unlabeled solutions containing the test concentrations of N. Second, teabags containing roots were placed in a solution similar to the previous one except that N forms were ^{15}N-labeled. Corresponding concentrations of ^{15}N forms ($K^{15}NO_3$, $(^{15}NH_4)_2SO_4$, or ^{15}N-glycine) were used. Roots were bathed in those solutions for 10 min (Kronzucker et al. 1995a, 1995b). Third, two washing steps were performed, both in N solutions identical to those used for acclimation. The first step lasted 5 s and freed roots of labeled N adsorbed on root surfaces. The second one lasted 2 min and removed apoplastic ^{15}N. Timing was based on efflux studies to exclusively measure influx (Kronzucker et al. 1995a, 1995b, Britto et al. 2000). All solutions (pH adjusted to 6.5) were air-bubbled to ensure oxygenation and homogeneity of nutrient availability. Laboratory temperature averaged 20–25 °C. Finally, labeled samples were cut Manually into smaller pieces and transferred into 10 mL plastic tubes and dried for 72 h at 60 °C. An automated ball mill was used to obtain 3–4 mg of root powder, which was placed in pewter microcapsules. Isotope-ratio mass spectroscopy analysis of total N content and ^{15}N abundance was carried out by INRAE SILVATECH (Silvatech, INRAE, 2018; Structural and functional analysis of tree and wood facility, https://doi.org/10.15454/1.5572400113627854E12). Analysis of nitrogen isotope composition $d^{15}N$ and nitrogen and carbon contents were performed by placing tin capsules containing dry material in an elemental analyzer (vario ISOTOPE cube, Elementar, Langenselbold, Germany) coupled, via a gas box interface, to a continuous flow isotope ratio mass spectrometer (Isoprime100, IRMS, Elementar UK, Cheadle, UK) available at SILVATECH. The sample was burned at 1025 °C in excess of oxygen. Then, the NOx were reduced using a quartz tube filled with copper heated at 650 °C. CO_2 was trapped at 35 °C by an adsorption column while N_2 passed through the thermal conductivity detector (TCD). Next, CO_2 was released from the adsorption column at 225 °C. Elementary gases were analyzed and detected by isotope ratio mass spectrometry, Isoprime100 IRMS (Cheadle, UK). Carbon and nitrogen contents were expressed in % of dry matter. $d^{15}N$ is expressed as delta values in ‰ relative to air N_2. The $d^{15}N$ uncertainty of measurements is 0.5‰ (2σ) in nitrogen for complex samples (i.e., not pure molecules).

2.6 *Calculations of ^{15}N influx rates in oak roots*

Total N amounts (N_{tot}, [mg]) were calculated as follows:

$$N_{tot} = (\%N_{tot} \times DW_{roots})/100 \quad (3)$$

where $\%N_{tot}$ is the nitrogen content (% of dry weight, DW) and DW_{roots} is DW (mg) of the roots.

The amount of ^{15}N in the sample ($^{15}N_{amount}$, [µg]) was given by the equation:

$$^{15}N_{amount} = (IA_{sample} - IA_{reference}) \times N_{tot} \times 10 \quad (4)$$

using isotopic abundances of the labeled samples (IA_{sample}) and natural unlabeled ones ($IA_{reference}$). Isotopic abundance (IA) is the ratio of ^{15}N over total N present in the sample. This can be written:

$$IA = {}^{15}N_{amount} \times 100/N_{tot} \quad (5)$$

Influx rates of nitrate, ammonium, and glycine (I_{Nit}, I_{Amm}, and I_{Gly} respectively, [µmol h^{-1} g $(DW)^{-1}$]) were given by the following equation:

$$I = {}^{15}N \text{ amount} \times (IA_{\text{labelling solution}}/100) \times (1/MM^{15}N) \times (60/d) \times (1/DW_{roots}) \quad (6)$$

$IA_{\text{labelling solution}}$ is the isotopic abundance of the nutrient solution enriched with ^{15}N (atom-% = 99%). $MM^{15}N$ is the molar mass of the labeling isotope (in this case 15 g/mol), and d is the duration of the influx monitoring (10 min).

2.7 Identification of *Q. petraea* genes involved in N transport, assimilation, and vascular unloading

N-related metabolism was studied through the transmembrane uptake and assimilation processes of the two primary inorganic forms, nitrate (NO_3^-), and ammonium (NH_4^+). Finally, the release of nitrogenous metabolites (i.e., glutamine and asparagine) in the vascular system was assessed.

Putative *Q. rubra* genes (a species ontogenetically close to *Q. petraea*, as data were not available for *Q. petreae*, and specifically sought for this study) involved in the transmembrane diffusion and enzymatic assimilation of mineral nitrogen, followed by the release of nitrogenous metabolites into the vascular system, were retrieved from Phytozome (V13, https://phytozome-next.jgi.doe.gov/2023/11/28), using blast alignments (https://phytozome-next.jgi.doe.gov/blast-search) with known heterologous sequences from *Arabidopsis* (Heynh.) and *Populus* (L.), and basic searches by keywords. For each gene family, candidates were aligned to assign their potential subfamilies. Because our work focused on the general molecular responses developed by oak roots challenged by *M. caerulea* exudate, we prioritized the molecular investigation of genes that exhibited transcribed homologs in the NCBI EST libraries (https://www.ncbi.nlm.nih.gov/), or were identified as transcribed sequences in the Phytozome databases. A preliminary nomenclature was then attributed to each gene exhibiting transcribed homologs in the NCBI's public EST databases. The nomenclature is fully consistent with that traditionally assigned to each protein family and potential related subgroups. To unambiguously identify the transmembrane candidates, the helical transmembrane regions (TMHs) were predicted using the TMHMM-2.0 (www.cbs.dtu.dk/services/TMHMM/) (Sonnhammer et al. 1998). Likewise, the putative subcellular localizations were predicted using WoLF PSORT II (https://www.genscript.com/wolf-psort.html) (Horton et al. 2007), and Plant-mPLoc (http://www.csbio.sjtu.edu.cn/bioinf/plant-multi/) (Chou and Shen 2010). Predicted subcellular localization and presence of transmembrane helices of *Quercus rubra* transporters are summarized in Appendix Table 1.

2.8 Gene expression analysis by real-time RT PCR

Approximately 150 mg of root material was removed from each harvested oak seedling (see Section 2.2), gently washed, immediately immersed in liquid nitrogen, and stored at − 80 °C. Each sample was ground to a fine powder in liquid nitrogen. Total RNA was extracted with a CTAB extraction buffer (cetyltrimethylammonium bromide), as previously described in Lopez et al. (2012). The RNA concentration and purity were determined using a NanoDrop™ ND-1000 spectrophotometer (NanoDrop®, France), and RNA integrity was verified by 2% agar gel electrophoresis, staining with 10% (v/v) SYBR® Safe DNA gel stain (Invitrogen, Carlsbad, CA, USA). One microgram of total RNA extracted from each biological replicate was subsequently pooled to generate the five aforementioned biological replicates (see Section 2.2). First-strand cDNAs were synthesized from 2 µg of mixed total RNA, using SuperScript III (Invitrogen, Carlsbad, CA, USA), following the manufacturer's instructions, and stored at − 20 °C until use. Real-time quantitative PCR was carried out on an Applied Biosystems StepOnePlusTM Real-Time PCR System (Applied Biosystems, Foster City, CA, USA). The amplification reactions were performed in a 15 µL of final reaction mixture, including 1X of TakyonTM Rox SYBR® MasterMix dTTP Blue (Eurogentec, Liege Science Park, Belgium), 2 µL of 1:30 diluted cDNA, and 100 nM primers (Appendix Table 2). qPCR reactions were conducted according to the manufacturer's instructions, with the following conditions: pre-denaturing at 95 °C for 3 min, 35 cycles (95 °C for 10 s, 60 °C for 10 s, and 72 °C for 20 s), and 72 °C for 15 min. PCR reactions were ended by generating a dissociation curve of 60–95 °C, with an increment of 0.3 °C/15 s, to avoid primer dimers and nonspecific amplifications. Prior to qPCR with each primer pair, PCR conditions were determined by comparing threshold values in a dilution series (0, × 15, × 30, × 60) of a cDNA mix, generated with all RT products. For each gene, primer pairs were designed within consensus regions among homolog genes recovered from different oak species (NCBI), and the amplification efficiencies were calculated (Appendix Table 2). Transcript levels were

normalized to those of five *Quercus* encoding housekeeping genes: *translation elongation factor 1-alpha EF1α* (XP_050292676.1), *histone H4* (XM_024020482.1), *polyubiquitin 10* (JAAMOV010000008.1), *serine/threonine-protein phosphatase PP2A catalytic subunit* (XM_031100507.1), and *ribosomal protein S13 mRNA* (RPS13) (OW028771.1). These genes corresponded to the best-suited reference genes ($p < 0.001$) from eight widely used housekeeping genes. They were identified with the software application BestKeeper (Pfaffl et al. 2004). The BestKeeper Index was estimated and was used as a calibrator for calculating the transcript abundances. Each referrer belongs to protein families involved in different cell processes, to minimize the risk of co-regulations. The relative expression of nitrogen-target genes was evaluated by using the $2^{-\Delta\Delta Ct}$ method (Livak and Schmittgen 2001). For clarity, and especially for downregulated genes, values were graphically normalized to 0 (signifying no change in gene expression), where each unit on each side of 0 corresponds to a twofold increase and a twofold decrease, respectively. Overall constitutive transcript steady-state levels were assessed by comparison of the mean of the cycle threshold (Ct). The final results from each statistical output were plotted after distribution and assignation of a score value between 0 and 100, an arbitrary scoring range. A Ct of 20 was assigned an arbitrary value of 100 (corresponding to the highest gene expression level). A Ct of 40 was assigned an arbitrary value of 0 (no expressed gene). All other Ct were then assigned values between 0 and 100, scaled based on their relative distributions. We emphasize that the complexity of studying these large superfamilies (along with those presented below) was overcome by retrieving all related members from specialized public genomic resources, such as NCBI and Phytozome. Subsequently, the genes whose transcriptional expressions were monitored in our study corresponded either to genes identified as potentially transcribed (identifiable with the existence of transcribed sequences integrating non-coding regions on both sides of retrieved genes in Phytozome V13, and the presence of their homologs from various oak EST libraries in NCBI), or based on their ability to specifically transport nitrogen, as observed with some AQPs. Regarding these latter, NH_3 diffusion is confirmed for the TIP2 and NIP1 subgroups, which correspond to the tonoplast intrinsic protein and the nodulin 26-like major intrinsic protein subfamilies, respectively, and predicted for members of the *X*-intrinsic proteins (XIP) subfamily.

2.9 Statistical analyses

All tests were performed using R Studio software (2023.09.1 + 494 "Desert Sunflower," using R edition 4.3.1). Differences in oak height increments and relative budburst rates were analyzed with Wilcoxon's sum rank test. For the N uptake assay, a root teabag represents an experimental unit. The effect of the different factors (N concentration, N form, treatment with *M. caerulea* root exudates) and their interactions on the variable (influx) were tested on the entire data set. Significance levels were set to $\alpha = 5\%$. Normality conditions were verified with the Shapiro–Wilk test and QQ plots, and homoscedasticity with the Bartlett test. ANOVA was performed and statistical groups were established with Tukey's honestly significant difference test. Variation degree was calculated for each factor combination. Gene expression was analyzed with the Kruskal–Wallis test. The *p*-values were adjusted according to the Benjamini–Hochberg procedure (Benjamini and Hochberg 1995).

3 Results

3.1 *Molinia caerulea* root exudates reduced budburst and height growth in oak seedlings

The addition of *M. caerulea* root exudates caused a significant decrease in the relative budburst rate ($p = 0.021$, Fig. 1A, Appendix Fig. 5A). While control plants presented a mean relative budburst rate of 31% on the whole period, treated oaks averaged only about half of this value. By the end of the experiment (6 weeks after starting application of root exudate), 85% of control oaks and 62% of treated oaks displayed leaves.

The mean weekly relative height increment (RHI) showed a significant negative response to treatment ($p = 0.049$) (Fig. 1B, Appendix Fig. 5). While control plants displayed RHI of 1.58% ± 0.19 (SE), treated plants showed values of 1.00% ± 0.16 (SE). Absolute height values measured over time (Fig. 1, Appendix Table 3) showed a significant negative treatment effect beginning during the third week of the experience ($p = 0.004$), when control and treated plants measured 86.3 cm ± 1.72 (SE) and 81.5 cm ± 2.33 (SE), respectively.

3.2 Kinetics of root N influx responded to treatment with *Molinia caerulea* exudates

N influx rates responded to increasing substrate concentrations with a sharp increase from 50 to 500 µM N concentration in the nutrient solution ($p = 4.55 \times 10^{-10}$), followed by lower increase between 500 and 1500 µM in most observations approaching a plateau that theoretically situates at 1500 µM. Under both conditions (control and treated, Fig. 2), influx rate values varied according to the tested N chemical forms ($p = 2 \times 10^{-16}$) as follows: ammonium, glycine (tenfold decrease), and nitrate (40-fold decrease). No significant effect of exudate application was observed for either ammonium or glycine influx rates after application of *M. caerulea* root exudates, except at 500 µM NH_4^+, when the influx for the treated

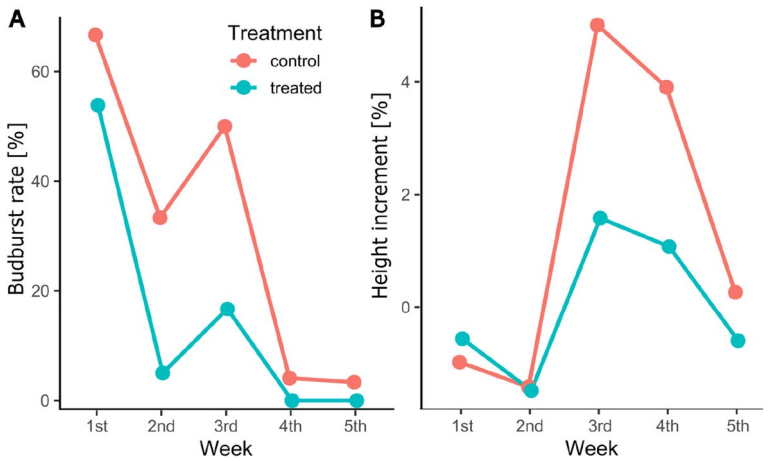

Fig. 1 Weekly evolution of (**A**) budburst rate and (**B**) height increment of oak seedlings beginning at first *Molinia caerulea* exudate treatment. Treatment group consisted of oak seedling irrigated with *M. caerulea* exudates while control oaks received distilled water instead

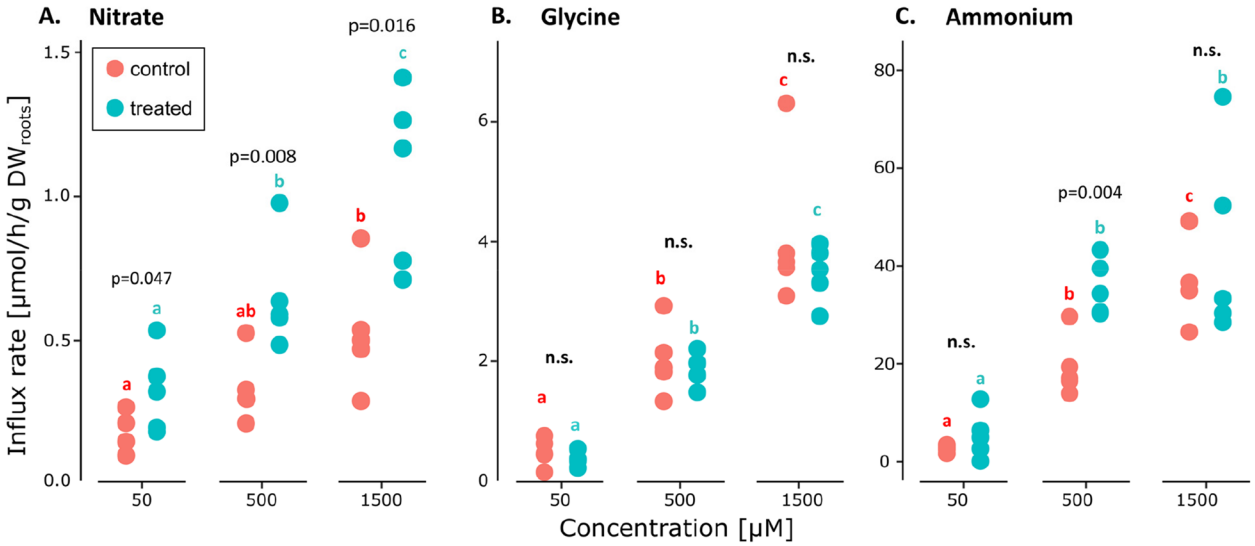

Fig. 2 Influx rates of nitrate (**A**), glycine (**B**), and ammonium (**C**) in excised fine roots of oak seedlings in response to different concentrations of nitrogen sources. *p*-values indicate significance of differences between treatments at the same concentration (n.s. = *p*-value above 0.05). Lowercase letters indicate significance levels between concentrations for the same treatment modality

exceeded the control ($p = 0.004$) (Fig. 2C). By contrast, applying exudates doubled nitrate influx rates compared to those measured in the roots of control plants, whatever the concentration (Fig. 2A).

3.3 The expression of genes related to nitrogen metabolism corroborated N influx rate pattern on application of *Molinia caerulea* root exudates

Transcriptomic analyses revealed a predominance of upregulated trends for NAR2, CLC, SLAH3, NIP1, TIP2, and XIP families (Fig. 3, Appendix Fig. 4). Expressions were more contrasted for the NPF, NRT2, and AMP families under our biological conditions, with significant upregulations (NPF1, NPF3, NPF6, NIP1a, XIP2, AMT11b, AMT13, AMT32, and AMT33a), downregulations (NPF4a and -b, NPF5c, NPF7, NRT2a, AMT11a, AMT12, and AMT31b), and non-modulated genes (NPF5b, NRT2b, AMT2, AMT31a, and AMT33b). In the roots of *Q. petraea*, some transporter-related genes were not transcribed, such as NPF2a and -b, NPF5a, NIP1b, and XIP1.

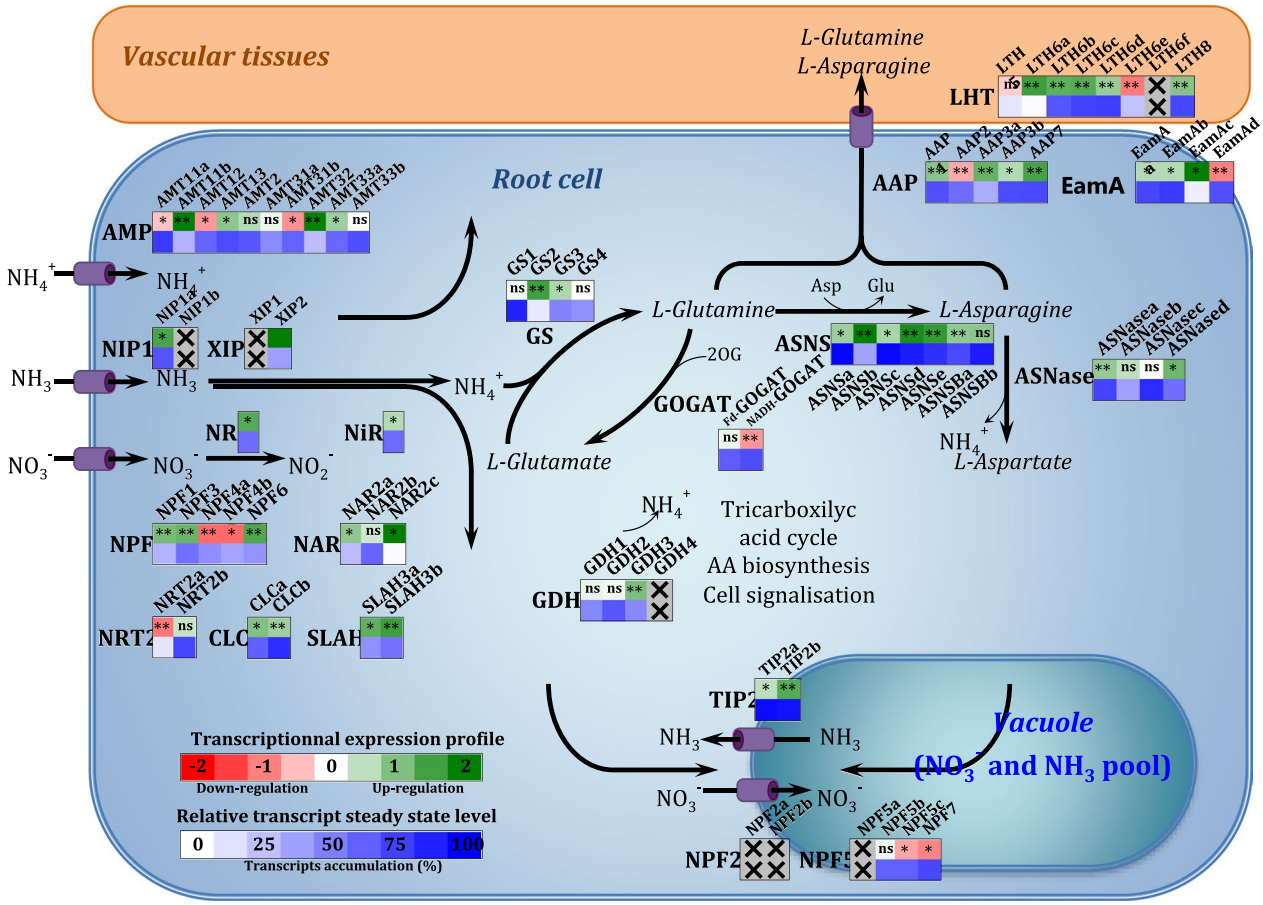

Fig. 3 Quantitative real-time RT-PCR of selected genes related to nitrogen transport, assimilation, and vascular release. Transcript abundances were recorded in root tissues of *Quercus petraea* seedlings at 6 weeks after treatment with *Molinia caerulea* exudates. Color scales represent level of transcriptional expressions (green, up-expression; red, down-expression), and the transcript steady state level (white, extremely low transcript accumulation; dark blue, maximal transcript accumulation). Genes with no transcription are indicated by a gray square with a black cross. The significant differences were statistically analyzed between untreated and treated roots with *M. caerulea* exudates. Each biological condition comprised five biological replicates, with each replicate representing a pooled sample of six randomly selected seedlings (Kruskal–Wallis, adjusted *p*-value < 0.05). Complete statistical data, including the SE and *p* values, are detailed in Appendix Fig. 4. * *p*-value < 0.05, and ** *p*-value < 0.01; "ns" indicates no significant difference between treatments. Values corresponding to the "Relative transcript steady state level" are detailed in Appendix Table 2. AAP-EamA-LHT, amino acid transporter; AMT, ammonia transporter; ASNase, asparaginase; ASNS, asparagine synthetase; CLC-SLAC-SLAH, chloride channel; GDH, glutamate dehydrogenase; GOGAT, glutamate synthase; GS, glutamine synthase; NIP, nodulin 26-like intrinsic proteins; Nir, nitrite reductase; NR, nitrate reductase; NAR-NRT-NPF, nitrate transporter; TIP, tonoplast Intrinsic proteins, XIP, X-intrinsic protein

Regarding genes involved in inorganic N assimilation, the number of members from each family was relatively restricted. The identification of genes encoding proteins involved in the GS/GOGAT pathway includes five glutamine synthase isoforms (three cytosolic isoforms with GS1, GS2, GS3; the chloroplastic GS isoform GS4; and a pseudogene), and three glutamate synthase (GOGAT) isoforms with two duplicated chloroplastic NADH-dependent glutamate synthase isoforms (NADH-GOGAT) and a ferredoxin-dependent amyloplastic (Fd-GOGAT). Glutamine (Gln) metabolism is closely connected to asparagine (Asn) metabolism, involving asparagine synthases (9 members), and asparaginases (4 members). Additionally, seven glutamate dehydrogenases were identified from the *Q. rubra* genome, with four members (GDH1 to GDH4), for which transcript accumulations were monitored in this work. Overall, transcript accumulations were significantly enhanced, except for NADH-GOGAT, which was downregulated. Certain members, namely GDH1, GDH2, Fd-GOGAT, GS1 and −4, ASNSBb, and ASNaseb and -c, did not show significant modulation in roots by *M. caerulea* exudates. No GDH4 transcripts could be detected under our biological conditions.

Lastly, three amino acid transporter families belonging to the AAAP superfamily (AAPs, LHTs, and the

EamA-like transporter family, also known as AtSIAR1/UnamiTs) were studied. These families include plasma membrane transporters that transport neutral amino acids, such as Gln and Asn. The diversity within these families is high, resembling that of the NPF or MIP superfamilies: AAPs with 83 putative members, 94 LHTs, and 70 EamAs. We focused on some members whose permease activity for Asn and/or Gln had been experimentally demonstrated in orthologs. As observed above, transcript accumulations were significantly enhanced, except for LTH6e, AAP2, and EamAd, which were downregulated. LHT5 and LHT6f were either unaffected by the treatment or not transcribed under our experimental conditions, respectively.

4 Discussion

M. caerulea root exudates affected the whole spring phenology of oak seedlings; budburst was reduced along with early growth reduction. Contrarily to our hypothesis, N uptake by root transport system was partly increased by *M. caerulea* root exudates, while the transcriptomic analysis confirmed strong modifications of the expression of genes associated with the whole N metabolism, indicating more indirect effects than expected.

4.1 Application of *M. caerulea* root exudates limited growth and budburst in oak seedlings

Exudates of *M. caerulea* roots were applied to investigate their allelochemical properties on oak seedling phenology and early growth. They affected oak height growth, confirming a allelopathic action like previously reported (Timbal et al. 1990). However, the effect on oak phenology was unexpected. We observed that the first significant differences on tree development appeared already 4 weeks after application of *M. caerulea* root exudates. In previous studies, effects were observed after 6 weeks (Fernandez et al. 2020). This suggests that allelopathic action of *M. caerulea* occurs more rapidly than previously demonstrated, pointing to a critical oak developmental period. Such responses might result from chemicals, or induced pH variations possibly modifying availability in soil anions and cations (Zambelli et al. 2025). Similar observations of phenological effects mediated by plant-plant allelopathy have been documented in other models, such as vanilla and beans exposed to allochemicals (Adiputra et al. 2019; Amini et al. 2013). However, to our knowledge, this is the first report of impeded tree phenology mediated by allelopathy in forest ecosystems.

4.2 Reduced budburst of oak seedlings did not result from a decrease in N uptake

Ammonium was the preferred N form taken up in oak seedling roots, followed by glycine, and lastly nitrate. These results are in line with those observed in *Q. suber* (Mata et al. 2000). According to Warren and Adams (2007), plants prefer N forms that are predominantly available in their natural habitats. Oaks interacting with moor grass are mainly found on acidic soils supplying nitrogen predominantly as ammonium (Koyama and Kielland 2022; Ma et al. 2021). Glycine transport values, particularly when compared with nitrate transport, underline the significant role of organic N sources in oak seedling nutrition, even if it is ten times less than ammonium. This role is emphasized in forest ecology (Farzadfar et al. 2021) particularly during the non-growing season and the leaf expansion in deciduous trees (Koyama and Kielland 2022; Ma et al. 2021). Despite knowledge about the depressive effects of *M. caerulea* exudates on oak morphological and phenological features, the findings regarding nitrogen uptake rates were unexpected: exudate treatment had no inhibitory effect on measured influx rates. Instead, it significantly stimulated nitrate uptake at all concentrations, increasing HATS and LATS activity. For ammonium supply, a significant increase was detected only at 500 µM, with higher values recorded for treated plants. For other concentrations, no differences were measured, which jeopardizes conclusions on ammonium HATS or LATS activity. No significant difference was found in measured glycine influx. Several hypotheses may be suggested to explain these physiological responses to root exudate application.

Possibly, the increase in nitrate, and to a lesser extent, in ammonium influx for treated seedlings, might result from an increase in N mineralization rate, leading to higher nitrate and ammonium concentrations in the soil after *M. caerulea* root exudate application (Chen et al. 2009). Measurement of N mineralization processes would be helpful to test this hypothesis. In this last study, the allelopathic action exerted by the invasive species *Mikania micrantha* (Kunth) led to increased soil nitrate and ammonium concentrations, benefiting *M. micrantha*. Here, as no measurement of inorganic N was made during the experiment in soil, induced soil nitrate and ammonium concentrations resulting in higher N influx rate may be hypothesized. However, transcriptomic analyses may suggest other hypotheses, although we note that the budburst reduction was not associated with a decrease in N uptake in oak roots.

4.3 *M. caerulea* exudates modulated the expression of genes encoding key enzymes in N metabolism

Increased nitrate influx may result from the observed enhanced expression of genes encoding plasmalemma transporters involved in HATS and LATS activities. By contrast, the expression profiles of ammonium transporters showed greater variability between members,

with many events of up- and downregulation. At a cellular level, the shift in transcription of genes coding for key enzymes in N metabolism after application of *M. caerulea* root exudates suggests an increase in the accumulation of glutamine, one of the key transport forms of N. The corresponding transporters are crucial for the uptake of inorganic N, and in our biological conditions, transcriptome analyses revealed a significant upregulation of most of them, whether putatively localized in the plasmalemma (NPF, NAR2, NIP1, CLC, SLAH, and XIP2), or tonoplast (NPF5 and −7, NRT2, TIP). These patterns echo those generally induced in some plant species grown under non-limiting N availability but challenged with various abiotic or biotic stresses, or during beneficial interaction with fungal ectomycorrhiza (ECM) or plant growth-promoting microorganisms (PGPMs). In these situations, "stress tolerance" correlates with fluctuations in NO_3^- and/or NH_4^+ availability, which in turn modulates transporter expression or activity (Calvo et al. 2019; Castro-Rodríguez et al. 2016; Ding et al. 2015; Selle et al. 2005). Transcriptional levels are not automatically correlated with those of their related proteins, but these modulated gene expressions indicate that the oak roots did respond to the presence of *M. caerulea* allelochemicals by modulating nitrate and ammonium uptakes and subcellular distributions. Expression of genes involved in the enzymatic assimilation of inorganic nitrogen is globally activated, resulting in the over-accumulation of Gln/Asn, a phenomenon accentuated by the inhibition of NADH-GOGAT expression. These gene expression profiles enhancing the Gln and Asn accumulations are consistent with previous studies, where N levels fluctuated during acclimatization of plants to various types of abiotic and biotic stress (Lea et al. 2007; Yin et al. 2022).

According to the upregulations of ASNases, which play a key role in Asp accumulation, we can conclude that oaks were stressed by root exposure to *M. caerulea* exudates. The expression of genes encoding ASNases, which play a key role in Asp accumulation, were significantly upregulated in roots challenged by *M. caerulea* exudates. Asparaginases are known to respond to various environmental cues, and influence the accumulation of Asn and its byproduct, Asp (Credali et al. 2013; Ivanov et al. 2012). Among the free cytosolic amino acids (AAs), L-aspartate (Asp) serves as a central building block in nitrogen and carbon metabolism, playing pivotal roles in various metabolic processes. Asp is therefore a biochemically active compound with pleiotropic functions, closely linked to stress phytohormones, which collectively drive the plant's responses to sudden stress and its acclimation to challenging environments (Han et al. 2021).

The transcript accumulation of AA transporters toward xylem vessels increased. Such changes decrease cellular concentration of AAs, which are known to exert negative feedback on inorganic N influx rate, thereby activating nitrate influx rates through increased transcription of nitrate transporters in our experiment. Some down regulated expression trends were observed among these transporters, such as for AMP11a, AMP12, AMP31b, NPF4ab, NRT2a, LTH6e, AAP2, and EamAd. We are unable to propose specific functional interpretations for each transporter isoform. However, besides the fact that the role of transporters in the regulation of nitrogen homeostasis under allelopathic stress is likely complex and still largely unknown, the overall transcriptomic response highlighted a fine tuning of their availability, contributing to the complex regulation of N flows between various compartments (apoplasm, cytosol, and subsequently the morphoplasm, or vacuole). It is apparent that their activities are significantly influenced either by direct interaction with allelochemicals or indirectly through their phytotoxic effects on the molecular environment of the cell as a whole, as discussed below.

4.4 Which mechanisms might be involved in the allelochemical effects on oak seedling development?

Correlation between reduction in budburst and changes in N uptake, as well as transcriptomics in N metabolism, does not link them in a straightforward manner; however, it sheds light on several innovative hypotheses.

Allochemicals have an effect on signal transduction pathways, with several members exerting direct negative effects on membrane fluidity and integrity (Shearer et al. 2012). This is attributed to their detergent properties and their ability to induce imbalances in the antioxidant system, resulting in rapid production of reactive oxygen and nitrogen species (RONS), and the inhibition of the activity of various antioxidant enzymes at the contact area. The solubilization and peroxidation of phospholipids directly impact the membrane potential and fluidity, which ultimately affect primary functions such as signaling and transport. Identifying *M. caerulea* allelochemicals and testing their regulatory action (or "toxicity") on various key transporters would be of great interest. In any case, the upregulation of the N metabolism can be observed in connection with the plausible oxidative stress elicited by the *M. caerulea* exudates. Interestingly, Gln metabolism is essential for maintaining cellular redox homeostasis by harnessing enhanced RONS levels through the biosynthesis of glutathione, a major antioxidant tripeptide (Glu–Cys–Gly) that deactivates peroxide-free radicals in cells (Amores-Sánchez and Medina 1999; Liao et al. 2022). Likewise, Gln is required to detoxify some toxic metabolites by conjugation (Cook 2019; Tao et al. 2022). Similarly, Asp and its derivative

compounds are among the key bioprotectants for reconfiguring the overall metabolic network to help plants respond to stress, recover, and acclimatize in the long term (Lehmann et al. 2009).

In the same line, the increase in N uptake potential of oak roots could be part of the adaptive response of oak seedlings to the stress induced by the understory species. However, in spring, to ensure budburst, stored N compounds are hydrolyzed and transported in the form of amino acids (asparagine and glutamine in most cases) toward growing buds. The decreased relative budburst rates of treated oaks therefore suggest that the reinforced conservation strategy also encompasses an inhibition of the remobilization of the stored N, or that oaks loose greater amounts of N than they take up during the winter despite a reinforced conservation strategy, potentially due to unfavorable facilitation of *M. caerulea* N supply (Fernandez et al. 2020).

5 Conclusion and perspectives

This molecular ecophysiology work is the first to report reduced budburst dynamics of oak seedlings caused by *M. caerulea* interference through water-based root exudates. At variance with an assumed decrease of root N uptake, uptake capacities of N sources were barely changed, and those of nitrate, and to a lesser degree ammonium, were even increased in treated seedlings. Moreover, *M. caerulea* root exudates induced a significant effect on overall nitrogen metabolism in oak roots suggested by the transcriptomic analysis. The specific ways in which allelochemicals affect the nitrogen metabolism are not yet elucidated, but our results suggest a general situation of stress caused by the *M. caerulea* root exudates. Our results point to a need to identify compounds with allelochemical properties acting on N metabolism, ultimately tree phenology.

The differential physiological responses derive from metabolic adjustments (biochemical and transcriptomic) linked to cellular nitrogen homeostasis, although further research will be required to elucidate the biological significance of the underlying metabolic and molecular mechanisms. Several primary diamide amino acids play a substantial role in the observed adjustments, such as Gln and Asn. Future studies will need to identify the key function of these diamides that may give protection against the emergence of these cellular disorders linked to allelopathic stress. More generally, they will need to address the importance of amino acid biosynthesis and transport processes in maintaining the physiological integrity and productivity of plants in situations of intra- and interspecific competition.

Appendix

Table 1 Predicted subcellular localization and presence of transmembrane helices of *Quercus rubra*'s transporters. Subcellular localization predictions were performed by using WolF PSORT server (https://wolfpsort.hgc.jp/). Abbreviations of protein localization sites in the dataset are as follows: *Plas*, plasma membrane; *ER*, endoplasmic reticulum; *Gol*, Golgi apparatus; *Pero*, peroxisomes; *Chlo*, chloroplasts; *Mito*, mitochondria; *Vac*, vacuole; *Cyto*, cytosolic. The number mentioned besides localization roughly indicates the number of the nearest neighbors to the query which localizes to each site, but is adjusted to account for the possibility of dual localization. The strongest occurrences are highlighted in bold. Transmembrane helices predictions were performed by using the TMHMM-2.0 software (https://services.healthtech.dtu.dk/services/TMHMM-2.0/). The presence of transmembrane helices was notified « PM+», without specifying the number of predicted TMHs, which requires dedicated molecular dynamics (MD) calculations

QrAAP1	**Plas: 9 (E.R.: 2, golg: 2, vac: 1)**	**PM+**
QrAAP2	**Plas: 5** (vac: 4, golg: 3, cyto: 1, extr: 1)	PM+
QrAAP3a	**Plas: 10** (E.R.: 2, extr: 1, vac: 1)	PM+
QrAAP3b	**Plas**: 10 (vac: 4)	PM+
QrAAP7	**Plas: 8** (vac: 4, E.R.: 1, golg: 1)	PM+
QrLTH5	**Plas: 6** (vac: 4, E.R.: 2, golg: 2)	PM+
QrLTH6a	**Plas: 10** (golg: 2, vac: 1, E.R.: 1)	PM+
QrLTH6b	**Plas: 10** (E.R.: 3, vac: 1)	PM+
QrLTH6c	**Plas: 12** (vac: 1, E.R.: 1)	PM+
QrLTH6d	**Plas: 10** (vac: 2, E.R.: 2)	PM+
QrLTH6e	**Plas: 9** (vac: 3, E.R.: 2)	PM+
QrLTH6f	**Plas: 14**	PM+
QrLTH8	**Plas: 10** (vac: 2, cyto: 1, E.R.: 1)	PM+
QrNIP1a	**Plas: 11** (vac: 2, golg: 1)	PM+
QrNIP1b	**Vac: 2** (plas: 2, E.R.: 1, golg: 1)	PM+
QrTIP2a	**Vac: 13** (plas: 1)	PM+
QrTIP2b	**Vac: 8** (plas: 6)	PM+
QrXIP1	**Plas: 12** (plas: 12, vac: 1)	PM+
QrXIP2	**Plas: 11** (plas: 11, golg: 2)	PM+
QrCLCa	**Plas: 10** (vac: 2, E.R.: 2)	PM+
QrCLCc	**Plas: 9** (vac: 3, golg: 2)	PM+
QrEamAa	**Plas: 10** (E.R.: 3, chlo: 1)	PM+
QrEamAb	**Plas: 10** (E.R.: 3, chlo: 1)	PM+
QrEamAc	**Plas: 10** (E.R.: 4)	PM+
QrEamAd	**Plas: 5** (vac: 3, E.R.: 3, golg: 2, cyto: 1)	PM+
QrNPF1	**Plas: 10** (E.R.: 2, nucl: 1, vac: 1)	PM+
QrNPF2a	**Plas: 8** (vac: 3, E.R.: 2, nucl: 1)	PM+
QrNPF2b	**Plas: 9** (vac: 2, chlo: 1, E.R.: 1, golg: 1)	PM+
QrNPF3	**plas: 10** (chlo: 1, nucl: 1, vacu: 1, pero: 1)	PM+
QrNPF4a	**plas: 9** (vac: 3, E.R.: 2)	PM+
QrNPF4b	**plas: 7** (vac: 3, E.R.: 2, cyto: 1, mito: 1)	PM+
QrNPF5a	**plas: 13** (vac: 1)	PM+
QrNPF5b	**plas: 14**	PM+
QrNPF5c	**plas: 12** (E.R.: 2)	PM+
QrNPF6	**plas: 13** (vac: 1)	PM+
QrNPF7	**plas: 11** (vac: 1, E.R.: 2)	PM+
QrNAR2a	**plas: 10** (vac: 3, E.R.: 1)	PM+
QrNAR2b	**plas: 8** (vac: 4, cyto:1, golg: 1)	PM+
QrNAR2c	**plas: 6** (vac: 5, cyto: 1, E.R.: 1, golg: 1)	PM+
QrNRT2a	**plas: 12** (chlo: 1, E.R.: 1)	PM+
QrNRT2b	**plas: 5** (E.R.: 3, vac: 2, chlo: 1, pero: 1, golg: 1)	PM+
QrSLAHa	**plas: 5** (E.R.: 3, nucl: 2, cyto: 2, vac: 2)	PM+

Table 2 Localization, sequence, PCR efficiency, and average Ct levels for primers used for qPCR amplification

Loci/standard code	Primers pairs (5′—3′)	PCR efficiency (*E*)	Average *Ct* level
Housekeeping genes			
EF1α: Translation elongation factor 1-alpha			
QrEF1a	GAACGGAGATGCTGGGATGGTGA/TTTCTTTGC AGCGGACTTGGTGA	1.82	20.7
TUB: Tubulin			
QrTUBa	CAATAACACAGCAGTAGCTGAGG/CAAGAGCAG CCAGATCTTCACG	1.97	23.62
UBQ: Polyubiquitin 10			
QrUBQ10	CTGCGATTGCGTGGAGGAATGC/CATCTTCAAGCT GCTTGCCTGC	1.8	24.84
PP2A: serine/threonine-protein phosphatase PP2A catalytic subunit			
QrPP2A	CAGGAGGTTCCACATGAAGGACC/GGGCTCTTG AAATCAGTGAGAGC	2.02	31.78
RPS13: Ribosomal protein S13 mRNA			
QrRPS13	GTTAGGGCTTGCTCCTGAAATTCC/GTCTTCTTG TAGTAGCGAGCAAGG	1.92	23.45
HIS: Histone H4 protein			
QrHIS4	CCCGCGATTCGTCGTTTGGCTCG/ACGACATCCATG GCCGTCACG	1.94	22.62
Ammonium transporters			
AMT: Ammonia transporter			
QrAMT1.1a	CCATAGCCGCCGCAGGAATCA/CCATCGGCGGAC CAGAACCAGT	1.80	21.89
QrAMT1.1b	GGGAGAACCGCAGTCACAACCAC/GCAAACCCA CCAAGCAAACCATTA	2.08	29.83
QrAMT1.2	CTGCAGCTGGTGGCCTTTCTTAC/CCGGTGGGCTTA GGATAGTCTGTT	2.08	24.71
QrAMT1.3	AAGAGTGGGCCGGTTTGATGT/CTTGGCTGGTGT TGGGATAGG	2.04	23.04
QrAMT2	TGGGGCGGTGGGTTTCTTTAC/CCTGACCAACCC ATCCACAATAG	1.97	23.77
QrAMT3.1a	GAGAGAGAGAGTTTGGTTG/GATGTGCCGGATTGG TAAG	1.85	27.22
QrAMT3.1b	TGAAATGGGCTGCACTACCTGAA/GACACCCCA ATGGAACAAGAACC	2.09	24.57
QrAMT3.2	TGCATTGTGGGGTGATGGAG/TGCGCTACATGGCAA AACATC	2.21	30.58
QrAMT3.3a	CTCTCGAGCCTGTTCCTACCTGTC/GAGCTGCAT CATCCCCAATCTT	2.19	24.82
QrAMT3.3b	GGCTGGGCTGCACTGGTAATG/GAGGTATGGGTG AGCAAAGAGTCC	2.14	23.23
NO3- transporteur			
NPF: Nitrate and peptide transporter			
QrNPF1	GTTGATAACCTTACCTCAAGAGGG/GTACCAGTT ATTGCAACTCTTGTCC	1.95	29.86
QrNPF2a	GGCTTTCTCAAACTATCTAAGTGC/CTTCTCAGA CTGCTTTGTTAATTTCC	nd	0
QrNPF2b	CACCAGAACAAAAAGCAGGCCTG/CATCCACAT AAGGCTCATCTTCC	nd	0
QrNPF3	TTTACTGGCTACTCACATTGTTGC/ACCCCAACT GTGCCTAAAGCTGC	2.16	25.43
QrNPF4a	GAGCTCCTTATTGGTCTCTTTGG/GTGAAGCGATAA TGGCTATAGTCC	2.04	27.37
QrNPF4b	AGCTCACTCCTTGTTTCCCTCG/TGTGGGTGGTCT TGTCGATATGAC	2.13	28.99

Loci/standard code	Primers pairs (5′—3′)	PCR efficiency (*E*)	Average *Ct* level
QrNPF5a	GGGGGTAAGAGCTGGATAGGC/CTAGAGGAGACT TGTCCAAGGC	nd	0
QrNPF5b	TCACCGAGGATGGATTCTAAACG/TCCCTTCAATTC TTCTGTAAGCAC	1.95	24.32
QrNPF5c	TAACCAAGAAGGGCGGACATGG/CCATTGAAGCTA CACCTTAACATCC	1.91	24.44
QrNPF6	GGAACCCAGGCAAAGGACAGC/CCTATTTAACTA ACCATGGAGAGG	1.86	27.85
QrNPF7	TATGAAGATATCAACTGAGGATCAC/ATGTCATCT TCCTCATCTGCCTC	1.91	22.79
NRT: NitRate transporter			
QrNRT2a	GATCCCGAGAAAGCCATTGAGG/AAGTTGACAATC TTATTTGTCATAATTAC	1.94	33.31
QrNRT2b	GGCGAATGCGACAGAAGAAGAG/TAGCTAAACATG TGCTGGTGAGG	1.76	22.62
NAR: Nitrate Assimilation Related protein			
QrNAR2a	ATTGAGGAACATGATGGAGATTCG/CTAAAATGG CACAAATTTCCATCC	1.78	30.49
QrNAR2b	GTTGAAAAGGAAGAAGAAGGTAGT/TCTTGGTCT ACTATCAATTCTAC	2.27	24.54
QrNAR2c	AATGTTGAAAAGGGAGAAGAGAGC/TTCACCTTA GTTCACCAATAATCTC	1.88	34.56
SLAH: slow anion channel associated homologues			
QrSLAH3a	GAGAAGACTTGTCAAAGAGAAAAAGCC/CAGAAA TTGTGACTATAGCTTCTG	2.03	27.58
QrSLAH3b	GGCTCTGTTTATAACAACTATCTGG/CACCTCTCT CAGAGCTTGGAGG	1.82	25.42
CLC: plasma membrane chloride channel			
QrCLCa	ATTGTACCTAAGTATGTAGCAGCC/GAAGACTCA GTTCTCCTTTTCTCC	1.84	24.35
QrCLCc	TGTTGTACCAAAGAGTCAAGGG/ACCGACTATCAA ACATTCAGTTGC	2.06	20.99
Assimilation			
NiR: Nitrite reductase			
QrNiR	AGATGTTTACAAGAAGGGTGTTCC/GAAACCCAT ACCATACCAAAACTATC	2.19	25.23
NR: Nitrate reductase			
QrNR	CACAGAAAGTATTCTGCGAGAGC/CGCCTCACTTCT AAAACTTGTTCC	1.92	25.11
GS: Glutamine synthase			
QrGS1	GCGCCGTCTCACTGGCCGAC/CCTAAATGCAGG TGGGTGTAGC	2.25	20.25
QrGS2	CAAAAMAGCCATTGAAAAGCTCRAGT/ACAGGT TGAATAAATCTTCTTTATGG	1.99	33.52
QrGS3	GCAATTYTGAACCTGTCACTTCGC/GCTAGAGCT TCAGCCTCCAGTG	2.08	26.77
QrGS4	ATAGTTGCTGCTGGCATTGATGG/CAGAACATAATC AGCTTAATATCGG	2.16	27.62
GS: Glutamine synthase			
QrfdGOGAT	CTGGGAGCAGTAAAGGTTCTGC/TTCAGTGCTGGT CTCAGGGTAC	2.02	24.14
QrNadhGOGAT	CTGAAGGYCGGCAAGCTGCTGCA/GACGTCACC TATGTCATTACAGTG	1.94	23.19
GDH: Glutamate dehydrogenase			
QrGDH1	AGAGCCCTCAAAGCAGCTACTG/CAATAGTAATTG TGCCTAATTCTTTGG	1.87	27.04

Loci/standard code	Primers pairs (5′—3′)	PCR efficiency (*E*)	Average C*t* level
QrGDH2	GAAAGTGAACAATGAGCTGAAAACT/GAATATGGT TGAGAATCATTGGAGCC	2.13	23.76
QrGDH3	GTGGGATGAAGAGAAGGTAAATAGG/AAGGTTGAA GATGAATSAGAAATGG	1.87	27.03
QrGDH4	TGAGGAGGGCTTTCCATGAAATC/GGATGATAACCT YTGGATGCATC	nd	0
ASNase: Asparaginase			
QrASNasea	GATATTTTGGAAACTCTATGGAACG/ATTCCGAAT ATGAGCGAGGTTGC	1.90	25.39
QrASNaseb	TCATACGTGGGACCCTGGCTC/ACCCATCCTCAG TAGCACAACC	2.08	20.88
QrASNasec	CAAAGGAGAAGTCACAATGTCTTAT/AAGAGTGTG AGTGACTCACAGTG	2.10	28.73
QrASNased	AAAAGGAGAAGTTACAATGGCTTTG/GTCATTTGC CAAATACTAAGTGTAAG	1.94	22.54
ASNS: Asparagine synthetase			
QrASNSa	AGGATGCTTCTTCACATCGTCTG/CCCAATAATAAT GACAGCTATGC	2.05	18.39
QrASNSb	GGGTGCATTTTCACGAATGGAAGT/AACACAGTT TGATTACCAGCTTGC	1.97	28.80
QrASNSc	AGGATGTTTCTTCTCAACAGCAGT/ATACATTTTGTT TGTCAAGTGTCC	2.06	18.49
QrASNSd	AGGGTGTATGTTCCACAGTGG/CAGCAGCTAAGC TATTGAGAATCG	1.77	19.81
QrASNSe	AGCATGTTCCACAGTCAGAATGG/TCTGTGTCAGGA ATTAATGTGAGC	2.18	21.15
Aqua-ammoniaporines			
NIP: Nodulin 26-like intrinsic proteins			
QrNIP1a	CGTGAGATCACGACGAGTGGC/TTTCGCTATAGTTAT ATCCATAAAGG	1.84	23.58
QrNIP1b	CCGAGATCACCGAGCCTAAATC/CGGAGCAATCAC TAAACAAGTTCC	nd	0
TIP: Tonoplast intrinsic proteins			
QrTIP2a	ATTCGTCACAAATGGAGAGAGCG/CGGGTTCAT CGACCCACCACTA	2.11	18.72
QrTIP2b	GCAGTCACTGGAGGCTTGGCAA/GTTCATTGATCC ACCGGAGAATGG	1.67	19.12
XIP: *X*-intrinsic proteins			
QrXIP1	GGTGCAAGGAACTTGACATAACG/AAGAATAGT GGGATTATCATTTTTCC	nd	0
QrXIP2	GGGCCTGCTATTGCATGTGTGGC/TTTCTTCACTTC TTGTGAGCATGG	1.87	28.51
N-organic diffusion—Amino acid permeases			
AAP: amino acid permeases			
QrAAP1	CAAGTTCATCACAAGTGAGCATGC/GAAATTGAA ACCAGGTCTTGAACG	2.48	23.34
QrAAP2	TTGGAGAACCATGTTCGTGATGTT/AGACAGCCA GATAGTGTTCAAGC	2.62	25.30
QrAAP3a	TTGTAACAGCAGAATATGACATACC/CCATGGTTC TCTCTTAGTAACTGG	1.96	29.53
QrAAP3b	ATGGAGGTCAATTTTTGTGGTTGC/AACTTCAAC CTAATAGATGGCTGC	2.17	23.00
QrAAP7	TGGCTTTGTACATAATTTCTACACC/AATTACAGTAAT GCCTCAACTCAG	1.84	22.85

Loci/standard code	Primers pairs (5′—3′)	PCR efficiency (*E*)	Average C*t* level
EamA-like: Amino acid bi-directional transport (eq. MtN21/EamA-like/UMAMIT family)			
QrEamAa	AGCCATTGAAGAACCTGAAGCAG/CCACGTCCA CCATGCAACAATGC	1.95	22.70
QrEamAb	CAAGACGATGACAAAAGTGGAACC/ATATTCAAA GCAGTTCCACTAGG	2.01	21.84
QrEamAc	TAAAAGCAAAGATTACAAGTCCTCG/TGTTGCAGA GGTGCATGGAACC	2.02	34.02
QrEamAd	ATACCAGATGTCATAAAGAGTACAC/CAATGCATC CATTTTGATAATTATGG	2.26	23.35
LTH: lysine-histidine-like transporters			
QrLTH5	GGACGAGCCCTACGCCTCGC/ATAATAATTAAATCT AGTGACACAAAAG	1.97	33.14
QrLTH6a	CCAGGAATTGCACTCAGACTC/GTCATCAGGGAA ATGAGTTTAGCTT	1.78	34.71
QrLTH6b	CCAGGAATTGCACTCAGACTC/TCATCAGAAAAA TGAGTTCAGCCA	2.28	23.64
QrLTH6c	CTACAAGTACTCTGCGTTTCATTA/CCTTTATCTAAA AGGATTGCATTTGC	2.29	22.41
QrLTH6d	CCACAAGAATACTTCGGTTTACTG/TAACAGCAG CAGACTTCTCTTGG	2.09	22.15
QrLTH6e	GCCGACTAAGTTCCTTCGTTTCC/GGAACAAAGCAT TTTGTACCATCC	2.24	30.94
QrLTH6f	AAGTTCAAACCATCTTTCATACTCC/CTATCATCT GATTCTGAACTAATGC	nd	0
QrLTH8	CTCTTCCAGTCACATTTGCTTACC/AACATTCGTTAT GCAGAACTCAGG	1.99	24.01

Table 3 Absolute height of oak seedlings throughout the experiment with *Molinia caerulea* exudate treatment (cm, means ± standard-error, $n = 50$)

Week after treatment	Control	Treated	*p*-value
1	83.38 ± 13.81	79.38 ± 15.98	0.082
2	83.72 ± 13.67	79.88 ± 15.95	0.104
3	83.94 ± 13.83	80.12 ± 16.15	0.105
4	86.7 ± 14.05	81.5 ± 16.29	0.029
5	89.26 ± 14.46	82.68 ± 16.24	0.021
6	90.3 ± 14.32	83.14 ± 16.01	0.013

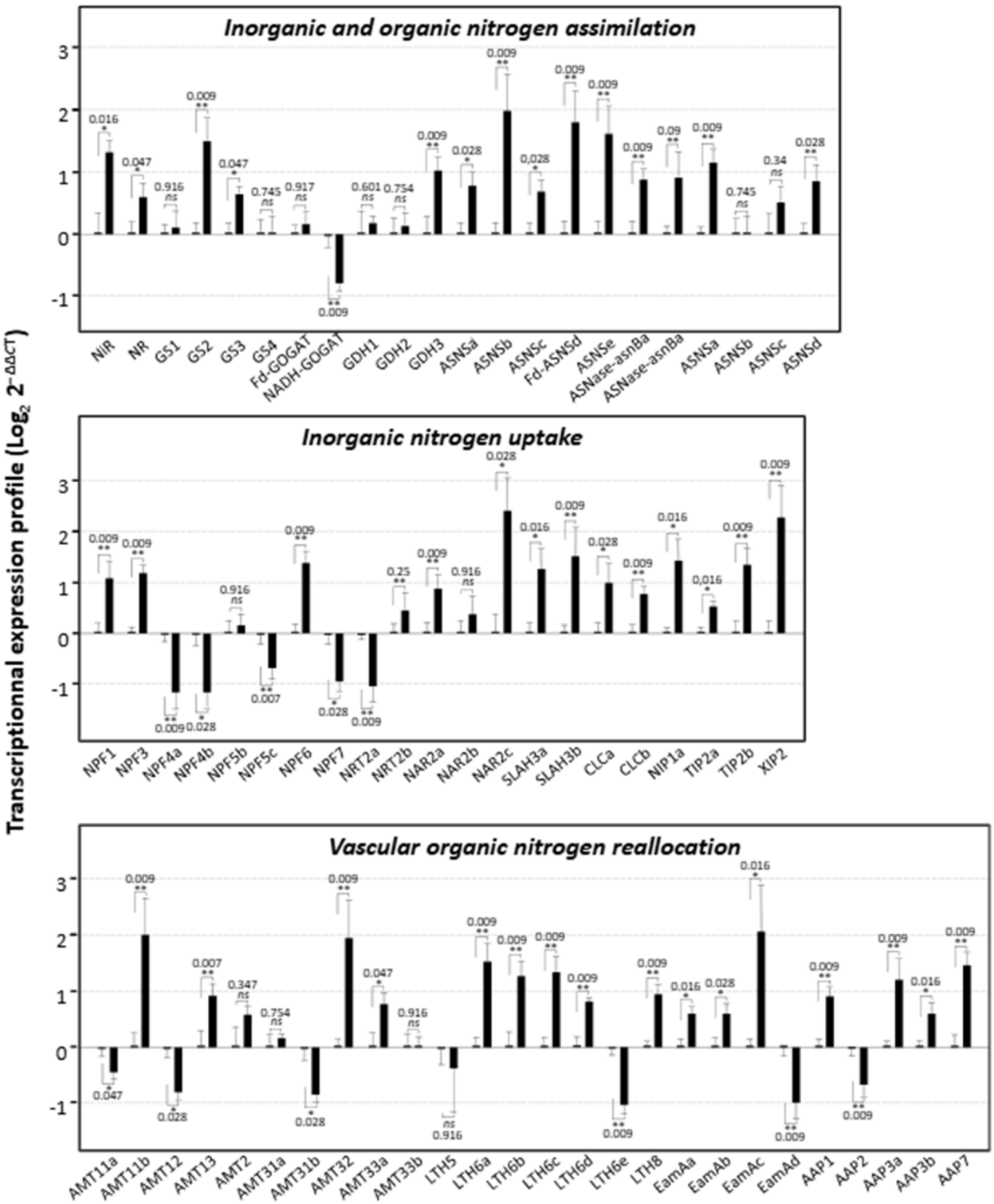

Fig. 4 Quantitative real-time RT-PCR of selected genes related to nitrogen transport, assimilation, and vascular release. Transcript abundances of the genes were recorded by real-time *q*RT-PCR analyses, relative to those of the control, using the $2^{-\Delta\Delta C.T}$ method. The significant differences were statistically analyzed between untreated and treated roots with *Molinia* exudate. Each biological condition comprised five biological replicates, with each replicate representing a pooled sample of six randomly selected seedlings (Kruskal & Wallis, adjusted *p*-value < 0.05)

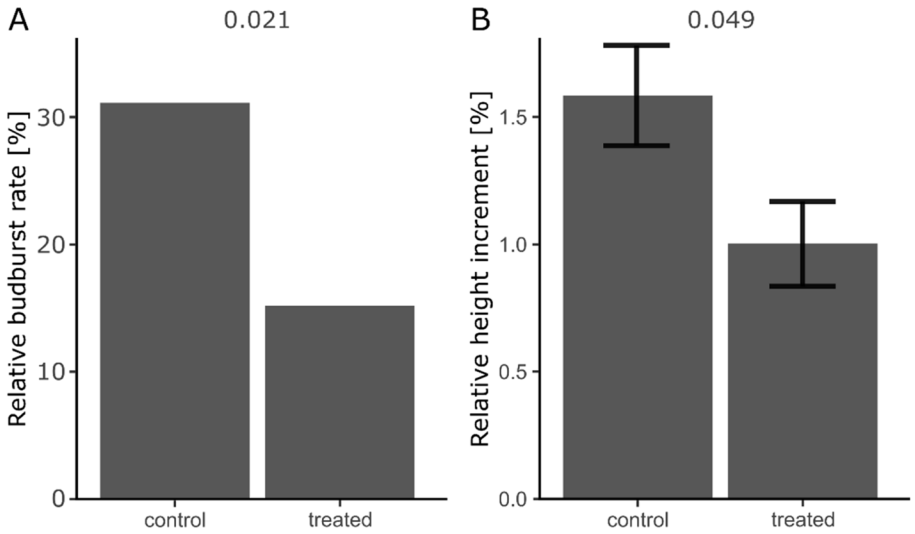

Fig. 5 Means of weekly relative budburst rate (**A**) and weekly relative height increment (**B**) of oak seedlings throughout the experiment. Treatment group consisted of oak seedling irrigated with *Molinia caerulea* exudates while control oaks received distilled water instead. *p*-values are given above figures. Bars represent standard errors

Acknowledgements
The authors thank SILVATECH (Silvatech, INRAE, 2018. Structural and functional analysis of tree and wood Facility, doi: https://doi.org/10.15454/1.5572400113627854E12) from UMR 1434 SILVA, 1136 IAM, 1138 BEF and 4370 EA LERMAB, localized at the research center INRAE Grand-Est Nancy, for isotope ratio mass spectroscopy analyses. The SILVATECH facility is supported by the French National Research Agency through the Laboratory of Excellence ARBRE (ANR-11-LABX-0002-01).

Authors' contributions
LA, PB, JSV, MF and PM have contributed to the conception and design of the work; LA, PB, JSV and PM have contributed to the acquisition of the data. LA and JSV analyzed data. LA, PB, JSV, MF and PM have contributed to interpretation of data; LA and JSV have drafted the work. MF, PB and PM have substantively revised it. PB and PM have supervised the project.

Data availability
Supplementary data is accessible at https://doi.org/10.57745/HEZHBC.

Declarations

Competing interests
The authors declare no competing interests.

Author details
[1]University of Clermont Auvergne, Clermont-Ferrand, France. [2]National Research Institute for Agriculture, Food and Environment, Paris, France.

Received: 31 January 2025 Accepted: 9 August 2025
Published online: 18 September 2025

References

Adiputra IGK, Winaja IW, Sumarya EM (2019) Vegetative growth of vanilla cuttings after addition of weed clippings mulch under 2 climatic condition, wet and dry seasons. IOP Conf Ser: Earth Environ Sci 399:012084. https://doi.org/10.1088/1755-1315/399/1/012084

Amini R, Ghanepour F, Movahedpou F (2013) Morpho-physiological and phenological changes induced by smooth amaranth allelopathic effects in various types of dry bean. Int J Agr Crop Sci 5(2):120–124

Amores-Sánchez MI, Medina MÁ (1999) Glutamine, as a precursor of glutathione, and oxidative stress. Mol Genet Metab 67:100–105. https://doi.org/10.1006/mgme.1999.2857

Becker M, Levy G (1983) Installation et dynamique d'une population de semis de chêne en milieu hydromorphe sous l'influence de divers facteurs (lumière, régime hydrique, compétition herbacée). Oecol Plant 4:299–317

Benjamini Y, Hochberg Y (1995) Controlling the false discovery rate: a practical and powerful approach to multiple testing. J Roy Stat Soc: Ser B (Methodol) 57:289–300. https://doi.org/10.1111/j.2517-6161.1995.tb02031.x

Boss WF, Mott RL (1980) Effects of divalent cations and polyethylene glycol on the membrane fluidity of protoplast 1. Plant Physiol 66:835–837. https://doi.org/10.1104/pp.66.5.835

Britto DT, Glass ADM, Kronzucker HJ (2000) Studies of nitrogen absorption and assimilation in plants by use of ^{13}N. In: Stevenson NR (ed) Proceedings of the 3rd International Conference on Isotopes: isotope production and applications in the 21st century. World Scientific Publ Co Pte Ltd, Singapore, pp 433–435

Calvo P, Zebelo S, McNear D et al (2019) Plant growth-promoting rhizobacteria induce changes in *Arabidopsis thaliana* gene expression of nitrate and ammonium uptake genes. J Plant Interact 14:224–231. https://doi.org/10.1080/17429145.2019.1602887

Castro-Rodríguez V, Assaf-Casals I, Pérez-Tienda J et al (2016) Deciphering the molecular basis of ammonium uptake and transport in maritime pine. Plant Cell Environ 39:1669–1682. https://doi.org/10.1111/pce.12692

Chen B-M, Peng S-L, Ni G-Y (2009) Effects of the invasive plant *Mikania micrantha* H.B.K. on soil nitrogen availability through allelopathy in South China. Biol Invasions 11:1291–1299. https://doi.org/10.1007/s10530-008-9336-9

Chou K-C, Shen H-B (2010) Plant-mPLoc: a top-down strategy to augment the power for predicting plant protein subcellular localization. PLoS One 5:e11335. https://doi.org/10.1371/journal.pone.0011335

Clark SL, Schlarbaum SE, Keyser TL et al (2016) Response of planted northern red oak seedlings to regeneration harvesting, midstory removal, and prescribed burning. Gen Tech Rep South Res Stn USDA for Serv 212:457–464

Cook SD (2019) An historical review of phenylacetic acid. Plant Cell Physiol 60:243–254. https://doi.org/10.1093/pcp/pcz004

Crawford NM, Glass ADM (1998) Molecular and physiological aspects of nitrate uptake in plants. Trends Plant Sci 3:389–395. https://doi.org/10.1016/S1360-1385(98)01311-9

Credali A, García-Calderón M, Dam S et al (2013) The K+-dependent asparaginase, NSE1, is crucial for plant growth and seed production in *Lotus japonicus*. Plant Cell Physiol 54:107–118. https://doi.org/10.1093/pcp/pcs156

Ding L, Gao C, Li Y et al (2015) The enhanced drought tolerance of rice plants under ammonium is related to aquaporin (AQP). Plant Sci 234:14–21. https://doi.org/10.1016/j.plantsci.2015.01.016

Farzadfar S, Knight JD, Congreves KA (2021) Soil organic nitrogen: an overlooked but potentially significant contribution to crop nutrition. Plant Soil 462:7–23. https://doi.org/10.1007/s11104-021-04860-w

Fernandez M, Malagoli P, Gallet C et al (2021) Investigating the role of root exudates in the interaction between oak seedlings and purple moor grass in temperate forest. For Ecol Manage 491:119175. https://doi.org/10.1016/j.foreco.2021.119175

Fernandez M, Malagoli P, Vernay A et al (2020) Below-ground nitrogen transfer from oak seedlings facilitates *Molinia* growth: ^{15}N pulse-chase labelling. Plant Soil 449:343–356. https://doi.org/10.1007/s11104-020-04473-9

Fernandez M, Vernay A, Henneron L et al (2022) Plant n economics and the extended phenotype: integrating the functional traits of plants and associated soil biota into plant–plant interactions. J Ecol 110:2015–2032. https://doi.org/10.1111/1365-2745.13934

Han M, Zhang C, Suglo P et al (2021) L-aspartate: an essential metabolite for plant growth and stress acclimation. Molecules. https://doi.org/10.3390/molecules26071887

Hoffmann WA, Haridasan M (2008) The invasive grass, *Melinis minutiflora*, inhibits tree regeneration in a Neotropical savanna. Austral Ecol 33:29–36. https://doi.org/10.1111/j.1442-9993.2007.01787.x

Horton P, Park K-J, Obayashi T et al (2007) WoLF PSORT: protein localization predictor. Nucleic Acids Res 35:585–587. https://doi.org/10.1093/nar/gkm259

Ivanov A, Kameka A, Pajak A et al (2012) *Arabidopsis* mutants lacking asparaginases develop normally but exhibit enhanced root inhibition by exogenous asparagine. Amino Acids 42:2307–2318. https://doi.org/10.1007/s00726-011-0973-4

Jabran K, Farooq M, Aziz T, Siddique K (2013) Allelopathy and crop nutrition. Allelopathy: current trends and future applications 337–348. https://doi.org/10.1007/978-3-642-30595-5_14

Koyama LA, Kielland K (2022) Seasonal changes in nitrate assimilation of boreal woody species: importance of the leaf-expansion period. Trees. https://doi.org/10.1007/s00468-021-02259-9

Kronzucker HJ, Siddiqi MY, Glass ADM (1995a) Compartmentation and flux characteristics of ammonium in spruce. Planta 196:691–698. https://doi.org/10.1007/BF01106762

Kronzucker HJ, Siddiqi MY, Glass ADM (1995b) Compartmentation and flux characteristics of nitrate in spruce. Planta 196:691–698. https://doi.org/10.1007/BF00197333

Lea PJ, Sodek L, Parry MA et al (2007) Asparagine in plants. Ann Appl Biol 150:1–26. https://doi.org/10.1111/j.1744-7348.2006.00104.x

Lehmann M, Schwarzländer M, Obata T et al (2009) The metabolic response of Arabidopsis roots to oxidative stress is distinct from that of heterotrophic cells in culture and highlights a complex relationship between the levels of transcripts, metabolites, and flux. Mol Plant 2:390–406. https://doi.org/10.1093/mp/ssn080

Liao HS, Chung YH, Hsieh MH (2022) Glutamate: a multifunctional amino acid in plants. Plant Sci 318:111238. https://doi.org/10.1016/j.plantsci.2022.111238

Livak KJ, Schmittgen TD (2001) Analysis of relative gene expression data using real-time quantitative PCR and the 2− ΔΔCT method. Methods 25:402–408. https://doi.org/10.1006/meth.2001.1262

Lopez D, Bronner G, Brunel N et al (2012) Insights into *Populus* XIP aquaporins: evolutionary expansion, protein functionality, and environmental regulation. J Exp Bot 63:2217–2230. https://doi.org/10.1093/jxb/err404

Lucash MS, Eissenstat DM, Joslin JD et al (2007) Estimating nutrient uptake by mature tree roots under field conditions: challenges and opportunities. Trees 21:593–603. https://doi.org/10.1007/s00468-007-0160-0

Ma WT, Tcherkez G, Wang XM et al (2021) Accounting for mesophyll conductance substantially improves ^{13}C-based estimates of intrinsic water-use efficiency. New Phytol 229:1326–1338. https://doi.org/10.1111/nph.16958

Mallik AU (2003) Conifer regeneration problems in boreal and temperate forests with ericaceous understory: role of disturbance, seedbed limitation, and keytsone species change. Crit Rev Plant Sci 22:341–366. https://doi.org/10.1080/713610860

Mata C, Van Vemde N, Clarkson DT et al (2000) Influx, efflux and net uptake of nitrate in *Quercus suber* seedlings. Plant Soil 221:25–32. https://doi.org/10.1023/A:1004785331462

Millard P, Grelet G (2010) Nitrogen storage and remobilization by trees: ecophysiological relevance in a changing world. Tree Physiol 30(9):1083–1095. https://doi.org/10.1093/treephys/tpq042

Nilsson MC, Zackrisson O (1992) Inhibition of Scots pine seedling establishment by *Empetrum hermaphroditum*. J Chem Ecol 18:1857–1870. https://doi.org/10.1007/BF02751109

Pfaffl MW, Tichopad A, Prgomet C, Neuvians TP (2004) Determination of stable housekeeping genes, differentially regulated target genes and sample integrity: Bestkeeper – excel-based tool using pair-wise correlations. Biotechnol Lett 26:509–515. https://doi.org/10.1023/B:BILE.0000019559.84305.47

Scavo A, Abbate C, Mauromicale G (2019) Plant allelochemicals: agronomic, nutritional and ecological relevance in the soil system. Plant Soil 442:23–48. https://doi.org/10.1007/s11104-019-04190-y

Schuler JL, Robison DJ (2010) Performance of northern red oak enrichment plantings in naturally regenerating Southern Appalachian hardwood stands. New Forest 40:119–130. https://doi.org/10.1007/s11056-009-9187-y

Selle A, Willmann M, Grunze N et al (2005) The high-affinity poplar ammonium importer PttAMT1.2 and its role in ectomycorrhizal symbiosis. New Phytol 168:697–706. https://doi.org/10.1111/j.1469-8137.2005.01535.x

Shearer TL, Rasher DB, Snell TW, Hay ME (2012) Gene expression patterns of the coral *Acropora millepora* in response to contact with macroalgae. Coral Reefs 31:1177–1192. https://doi.org/10.1007/s00338-012-0943-7

Shimoda K, Kimura K, Kanzaki M, Yoda K (1994) The regeneration of pioneer tree species under browsing pressure of Sika deer in an evergreen oak forest. Ecol Res 9:85–92. https://doi.org/10.1007/BF02347245

Simon J (2023) Relevance of organic vs. inorganic nitrogen in intra- and interspecific competition of seven central European tree species. Trees 37:1583–1591. https://doi.org/10.1007/s00468-023-02418-0

Sonnhammer EL, Von Heijne G, Krogh A (1998) A hidden Markov model for predicting transmembrane helices in protein sequences. Presented at the Ismb, pp. 175–182.

Tao CN, Buswell W, Zhang P et al (2022) A single amino acid transporter controls the uptake of priming-inducing beta-amino acids and the associated tradeoff between induced resistance and plant growth. Plant Cell 34:4840–4856. https://doi.org/10.1093/plcell/koac271

Thitithanakul S, Pétel G, Chalot M, Beaujard F (2012) Supplying nitrate before bud break induces pronounced changes in nitrogen nutrition and growth of young poplars. Funct Plant Bio 39:795–803. https://doi.org/10.1071/FP12129

Thomas FM, Blank R, Hartmann G (2002) Abiotic and biotic factors and their interactions as causes of oak decline in Central Europe. For Pathol 32:277–307. https://doi.org/10.1046/j.1439-0329.2002.00291.x

Timbal J, Gelpe J, Garbaye J, Courrier G (1990) Étude préliminaire sur l'effet dépressif de la molinie (*Molinia caerulea*) sur la croissance et l'état mycorhizien de semis de chêne rouge (*Quercus rubra*). Ann Sci Forest 47:643–649. https://doi.org/10.1051/forest:19900609

Vernay A, Balandier P, Guinard L et al (2016) Photosynthesis capacity of *Quercus petraea* (Matt.) saplings is affected by *Molinia caerulea* (L.) under high irradiance. For Ecol Manage 376:107–117. https://doi.org/10.1016/j.foreco.2016.05.045

Vernay A, Malagoli P, Fernandez M, et al (2019) Régénération du chêne en compétition avec la molinie : un délicat dosage des ressources en eau et en lumière. Les Rendez-vous techniques de l'ONF 3–10.

Wang Y-Y, Hsu P-K, Tsay Y-F (2012) Uptake, allocation and signaling of nitrate. Trends Plant Sci 17:458–467. https://doi.org/10.1016/j.tplants.2012.04.006

Warren CR, Adams PR (2007) Uptake of nitrate, ammonium and glycine by plants of Tasmanian wet eucalypt forests. Tree Physiol 27:413–419. https://doi.org/10.1093/treephys/27.3.413

Watt AS (1919) On the causes of failure of natural regeneration in British oakwoods. J Ecol 7:173. https://doi.org/10.2307/2255275

Weise G (1960) Allelopathische Beeinflussung und Ökotypenbildung bei *Molinia caerulea* (L) Mench. Ber Schweiz Bot Ges 73:35

Yin H, Yang F, He X et al (2022) Advances in the functional study of glutamine synthetase in plant abiotic stress tolerance response. Crop J 10:917–923

Zambelli A, Nocito FF, Araniti F (2025) Unveiling the multifaceted roles of root exudates: chemical interactions, allelopathy, and agricultural applications. Agronomy 15(4):845. https://doi.org/10.3390/agronomy15040845
Zhang Z, Liu Y, Yuan L et al (2021) Effect of allelopathy on plant performance: a meta-analysis. Ecol Lett 24:348–362. https://doi.org/10.1111/ele.13627

Publisher's Note